Available online at www.sciencedirect.com

jmr&t Journal of Materials Research and Technology

www.jmrt.com.br

Original Article

Crystal growth behavior and phase stability of rare earth oxides (4 mol.% $GdO_{1.5}$-4 mol.% $SmO_{1.5}$) doped zirconia nanopowders

R. Mahendran[a,*], S. Manivannan[b], S. Senthil Kumaran[c], A. Vallimanalan[a], M. Murali[a], S. Gokul Raj[d], S. P. Kumaresh Babu[a]

[a] Department of Metallurgical and Materials Engineering, National Institute of Technology, Tiruchirappalli, 620015, Tamil Nadu, India
[b] Department of Mechanical Engineering, Karpagam Academy of Higher Education, Coimbatore, 641021, Tamil Nadu, India
[c] School of Mechanical Engineering, Department of Manufacturing Engineering, Vellore Institute of Technology, Vellore, 632014, Tamil Nadu, India
[d] Department of Physics, C. Kandaswami Naidu College For Men (CKNC), Chennai, 600 102, Tamil Nadu, India

ARTICLE INFO

Article history:
Received 12 December 2018
Accepted 20 September 2019
Available online 20 October 2019

Keywords:
Zirconia
Coprecipitation
Rare earth oxide
Phase transformation
Tetragonal
Activation energy

ABSTRACT

Nanocrystalline powders of 4 mol.% $GdO_{1.5}$-4 mol.% $SmO_{1.5}$ doped ZrO_2 (4Gd4SmSZ) has been synthesized by co-precipitation process. Their phase transformation and crystalline growth behavior was investigated by Thermo gravimetric-Differential Thermal Analysis (TG-DTA), X-ray Diffraction (XRD), Raman spectroscopy and High-Resolution Transmission Electron Microscopy (HR-TEM) after calcinations at different temperatures. The XRD, Raman spectra and HRTEM results confirm the nature of tetragonal zirconia (t-ZrO_2). The prepared 4Gd4SmSZ powders, remains in the single metastable tetragonal phase over the whole calcination temperature ranging from 873 K to 1273 K for 2 h. The crystallite size varies from 11.98 nm to 18.90 nm with increase of temperature from 873 K to 1273 K. The activation energy of the prepared powders at low temperature is considerably lesser than that at a higher temperature. The annealed 4Gd4SmSZ powders had shown excellent phase stability at 1573 K for 100 h.

1. Introduction

Zirconia (ZrO_2) shows good electrical, thermal and mechanical properties and it finds application in oxygen pumps and sensors [1,2], fuel cells [3,4] and thermal barrier coating (TBC) [5,6] applications. Zirconia has three polymorphs;room temperature monoclinic which is stable upto 1400 K, intermediate phase is tetragonal(t) and it is stable from 1400 K to 2570 K and the cubic(c) phase is stable between 2570 K and upto their melting point. The high-temperature t phase is the most important one from the standpoint of their structural engineering application where better mechanical properties are expected. However,an inherent drawback is theirpoor stabilityat low temperature. In order to stabilize the t phase at room temperature, stabilizers for ex., MgO, CaO, Y_2O_3 and other rare-earth oxides can be doped into zirconia. This non-transformable, supersaturated t phase is known as t'favorable

* Corresponding author.
E-mail: mahendran.meta@gmail.com (R. Mahendran).
https://doi.org/10.1016/j.jmrt.2019.09.058

for TBC application. When the t phase is sufficiently lean in stabilizers, it undergoes a diffusionless transformation to monoclinic while cooling from 1443 K to room temperature. This in turn results in a volume expansion of 5%. It is obvious that this volume expansion will be a factor for crack formation on the coatings and eventually spalls from the surface [7]. In recent years, so many researchers concentrate on the addition of rare earth oxides into zirconia to stabilize t or c phase at higher temperatures [8–11]. To produce nanosized powders, several techniques such as co-precipitation [8,12], hydrothermal [13,14], sol-gel methods [15,16] are available. Owing to their simplicity and easy handling, co-precipitation technique is useful for preparing chemically homogeneous,nanosized zirconia powders. In the present work, 4 mol % $GdO_{1.5}$-4 mol % $SmO_{1.5}$-ZrO_2 powders were prepared by co-precipitation process at pH 10.9–11.0 and then calcined at various temperatures, 573 K and then at 873 K to 1273 K with an increment of 100 K for 2 h to investigate their phase transformation and crystal growth behavior. The phase stability of prepared powders at 1573 K for 100 h is also investigated.

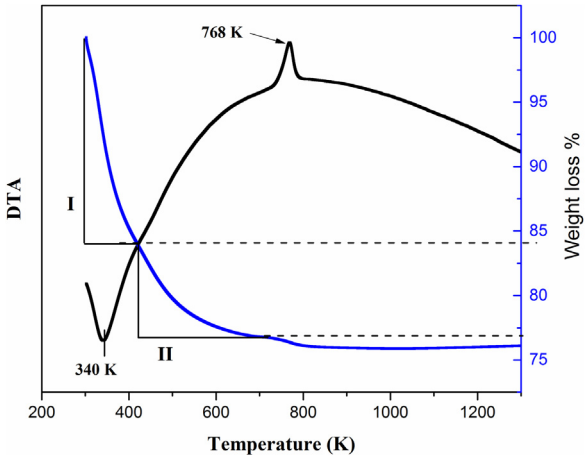

Fig. 1 – TG-DTA curve of 4Gd4SmSZ powders.

2. Experimental work

The starting materials are zirconium oxychloride octahydrate ($ZrOCl_2.8H_2O$), gadolinium nitrate hexahydrate ($Gd(NO_3)_3.6H_2O$) and samarium nitrate hexahydrate ($Sm(NO_3)_3.6H_2O$). The chemicals were purchased from Alfa-aesar, USA, with high purity of 99.99%. The chemical co-precipitation technique was adopted to prepare 4Gd4SmSZ powders. The respective nitrates and chlorideare taken in a stoichiometric ratio and mixed with deionized water to form a 0.3 M solution. The mixture solution was slowly added drop-wise to aqueous ammonia solution which is under stirred condition continuously with the use of magnetic stirrer Careful attention has been given to maintain the solution pH between 10.9–11.0 throughout the entire process. Over a short period of time, white precipitates gradually appear. After that the white precipitates were filtered and collected. Before collecting the precipitates, it was repeatedly washed with de-ionized water and ethanol. The filter precipitates were dried at 100 °C for 5 h in an oven. Finally the obtained product was ground with the help of agate mortar and pestle. Thereafter, calcination was done on the prepared powders at different temperatures for determining the phase transformation and activation energy. The performance of powders with respect to phase stability was evaluated by annealing them at 1573 K for 100 h in a box furnace. The powders were heat treated at a rate of 5 °C/min and furnace cooling was done. The powders were collected at different intervals to study the phase composition.

3. Characterization of the powders

TG-DTAanalysis was performed in nitrogen flow with a heating rate of 10 °C/min using simultaneous thermal analyzer (STA 8000, Perkin Elmer). FTIR (Spectrum-II, Perkin Elmer) was done on the as-prepared powders and the calcined samples (873 K to 1273 K) ranging from 1000 to 4000 cm^{-1} wave numbers. The structural characterization was carried out on the calcined powders by X-ray diffractometer (XRD - Rigaku Ultima III) with Cu Kα radiation at a wavelength (λ)=0.15406 nm). Scanning was done with 2θ range from 20 to 80°. Scherer formula [15] is used to estimate the average crystallite size of t-ZrO_2 and is given in eqn. (1),

$$D_t = \frac{0.89\,\lambda}{\beta\,Cos\,\theta} \quad (1)$$

where, D_t, λ, β and θ are the average crystallite size of t-ZrO_2, wavelength, full width at half maximum and diffracted angle. Micro Raman spectroscopy (Labram HR evolution, Horiba Jobin Yvon) was conducted and recorded at room temperature on the calcined powders in the spectrum range of 100 to 700 cm^{-1}. The microstructure of the calcined powders was characterizing dusing HR-TEM (JEOL, JEM 2100).

4. Results and discussion

4.1. *TG-DTA analysis*

Fig. 1 depicts the TG-DTA curve of 4Gd4SmSZ doped zirconia powders. As it can be seen, the weight loss (TG) curve exhibits two weight losses. The first one happens in the temperature range between 300.0 K and 421.0 K with a weight loss of 16.2%. The endothermic peak at around 340.0 K is assigned to the evaporation of absorbed moisture and water molecules present in the dried precipitates. The second weight loss of 7.4% occurs in between 421.0 K and 755 K, could be related with the decomposition of zirconium hydroxide formed during the precipitation process. After this stage, there was no weight loss displayed in TG curve. The DTA curve, revealed one single exothermic peak near 768.0 K, which may account for the formation of crystalline ZrO_2. After this, there are no apparent peaks present in DTA curve and no weight loss observed in TG curve.

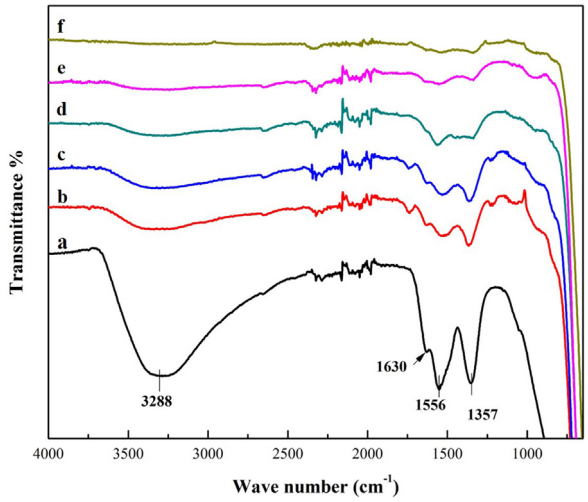

Fig. 2 – FTIR spectra of 4Gd4SmSZ powders a) as prepared b) 873 K c) 973 K d) 1073 K e) 1173 K and f) 1273 K.

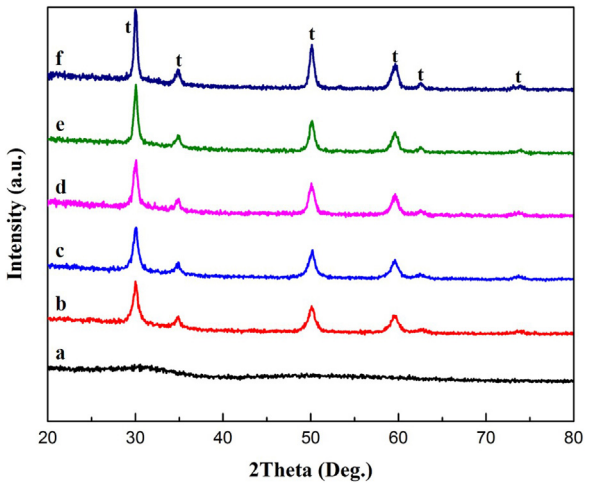

Fig. 3 – XRD pattern of 4Gd4SmSZ powders a)573 K b) 873 K c) 973 K d)1073 K e) 1173 K and f) 1273 K.

4.2. *FTIR analysis of 4Gd4SmSZ powders*

Fig. 2 shows the FTIR spectra of the as-prepared and the calcined 4Gd4SmSZ powders at different temperatures. It shows several bands appear in the range between 1000-4000 cm^{-1}. The band appearing at 3294 cm^{-1} corresponds to O—H stretching and the broadest nature is associated with hydrogen-bonded chains [17,18]. For the as-prepared dried precipitates the 3294 cm^{-1} band appears with higher intensity compared to the calcined powders. When the calcination temperature increases, the intensity of the band decreases and disappears at higher calcination temperatures. The band at 1626 cm^{-1} is another vibration band of water molecule which is arising from H—O—H bending bonds [19]. The band appearing at 1350 cm^{-1} and 1550 cm^{-1} represents the existence of nitrates and it belongs to the N–O asymmetrical stretches in the N–O bond [20,21].

4.3. *XRD pattern of 4Gd4SmSZ powders*

The X-ray diffraction pattern of the 4Gd4SmSZ powders is shown in Fig. 3. As can be seen from Fig. 3a (573 K), itreveals that the prepared powders are inamorphous condition indicating that crystallization does not take place. From Fig.1 the crystallization of t-ZrO_2has occurred well above 700 K which agrees with DTA result. From Fig. 3b (873 K), the reflection peaks corresponding to tetragonal zirconia (JCPDS: 50–1089) were identified and no other phases have been detected. As the calcination temperature is raised to 973 K, it is evident from Fig. 3c, that the prepared 4Sm4Gd-SZ powder remains in a single tetragonal phase. The XRD pattern shown in Fig.3d represents the powder calcined after 1073 K for 2 h, which results in increase of diffraction peak intensities with corresponding increase in calcination temperature. On raising the calcination temperature to 1173 K as shown in Fig. 3e, increase in crystallite size and crystallization occurred which is reflected in peak intensities and a decrease in Full width Half maximum was observed.

. Furthermore, the XRD pattern belonging to 1273 K (Fig. 3f) revealed that tetragonal was the dominant phase. It is reported, in a previous study by Hsu et al. [12], that t-ZrO_2 was formed between the calcination temperature 873 K and 1273 K inthe synthesized 3Y-TZP powders. In addition, they reported that intensity of the peak increases throughout the calcination temperature range without any new phase formation. Wang et al. [16] prepared 4 mol% yttria stabilized zirconia (4Y-TSZ) nanosized powders using coprecipitation technique and reported only t-ZrO_2. Once the powders calcined between 673 K and 1273 K, the reflection gets increased and they maintained the t-ZrO_2 phase over the calcination temperature. The present study agrees with the reports of Hsu et al. [12] and Wang et al. [16].

4.4. *Raman spectra of 4Gd4SmSZ powders*

Raman spectroscopy is very sensitive to local symmetry and it is widely employed to distinguish the different polymorphs of zirconia. The Raman spectra of 4Gd4SmSZ doped zirconia powders are represented in Fig.4. The peaks at 145, 260, 322, 467 and 635 cm^{-1}were assigned to the tetragonal mode of zirconia and it becomes stronger as the calcination temperature increases. The present result is further supported by the findings from Kim et al. [22], Qu and K.L. Choy [23] and Niu et al. [24]. The peak at 608 cm^{-1} could be hardly detected at higher temperatures. Moreover it could be pointed that no fingerprints of vibration modes belong to monoclinic polymorph was observed throughout the heat treatment range. This is consistent with the XRD result.

4.5. *Crystal growth behavior of 4Gd4SmSZ powders*

The crystallite size versus calcination temperature is represented in Fig. 5. From Fig. 5 it is observed that the average crystallite size increases with calcination temperature. When the precipitates were calcined at 873 K, the average crystallite size was about 11.97 nm and it grows to 12.74 nm after calcined at 973 K. It attains a value of 13.28 nm, when calcined at 1073 K.

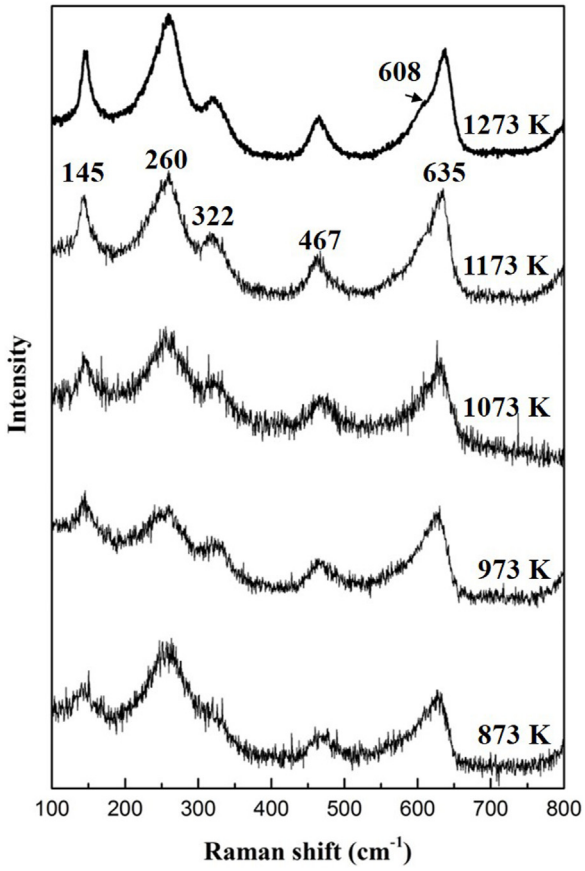

Fig. 4 – Raman spectra of 4Gd4SmSZ powders at various temperatures.

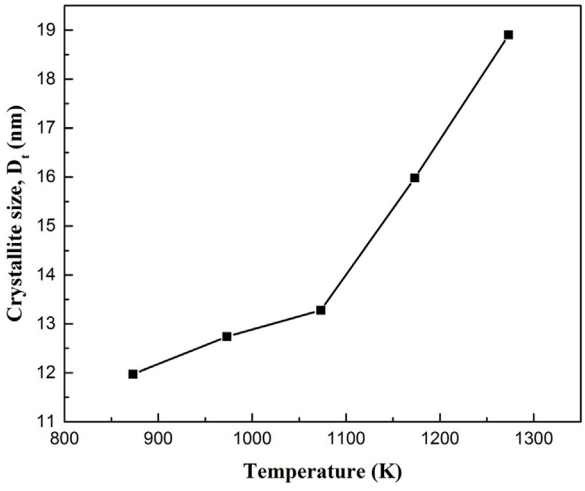

Fig. 5 – The evolution of crystallite size versus calcination temperature of 4Gd4SmSZ powders.

A further increase of temperature to 1173 K causes the crystallite size to reach 15.98 nm. Finally, it reaches around 18.90 nm, for 1273 K. These crystallite sizes are lower than the critical size of 30 nm, above which tetragonal to monoclinic(m) phase transformation can occur [25,26]. Also it is pointed out by Huang et al. [15] that smaller the particle size more stabilization could be achieved for t phase based on the nanoparticle

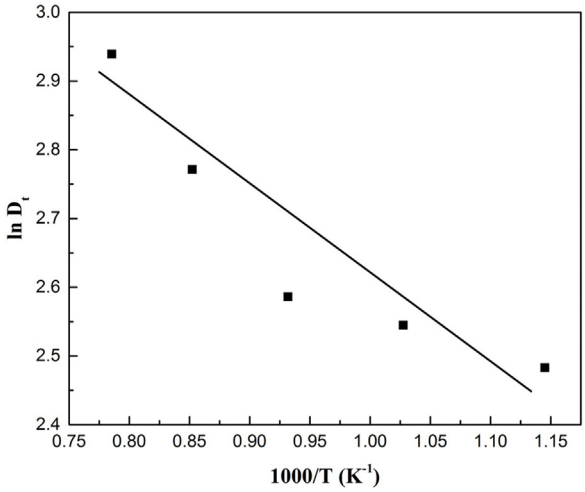

Fig. 6 – Relation between ln (D_t) versus 1000/T (K^{-1}).

size effect. Hence in the present study, no m phase transition occurred. XRD and Raman results support this understanding as in (Fig. 3&4).

The activation energy for crystallization was determined by Arrhenius equation [15], given below in eqn. (2)

$$D_t = k.\exp\left[\frac{\Delta E}{RT}\right] \quad (2)$$

where k is the constant value, R denotes the gas constant, D_t is the average crystal size and ΔE is the activation energy for crystallite growth. The lnD_t and the reciprocal of the calcination temperature was plotted in Fig. 6. From the slope, the activation energy for the t phase was calculated. The activation energy for the crystal growth, when calcined between 873 K–1073 K was found as 4.04 kJ/mol. and it was 20.04 kJ/mol. when calcined between 1073 K–1273 K. The activation energy was lower than that of 34 kJ/mol. [27], 29.2 kJ/mol [28]. and 24.79 kJ/mol. [29]. The reduction in activation energy in the present study is due to the presence of large vacancies within the nanocrystallites due to the incorporation Gd^{3+} and Sm^{3+}. Also, it is reported that, an increase in the concentration of oxygen vacancies may occur in nanocrystalline ceramic particle nanocrystallites if their particle size was less than 20 nm [30]. Therefore, due to these combined effect, 4Gd4SmSZ nanocrystalline powder experience comparative reduction in the activation energy

4.6. *Microstructure of the 4Gd4SmSZ powders*

SEM micrograph of 4Gd4SmSZ powders calcined at 1073 K is shown in Fig. 7a, which reveals the powder particles are in the form of large clusters. EDS measurement was taken on the calcined powders (1073 K) which is illustrated in Fig. 7b. It shows the presence of Zr, Sm and Gd constituents and no impurities were observed in the prepared powders which demonstrates the coprecipitation process reliability and the starting material purity.

Fig. 8a.shows the HRTEM images of powders calcined at 1073 K for 2 h. The powders are in agglomerated state. The

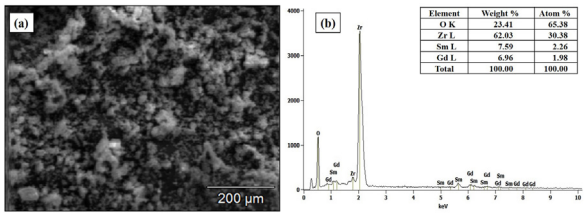

Fig. 7 – SEM micrograph of a) 4Gd4SmSZ powders calcined at 1073 K b) Energy-dispersive spectra showing the corresponding constituents.

agglomerated condition is due to the steps involved in the synthesis process. The SAED pattern shown in Fig. 8b, demonstrates that the prepared powders are polycrystalline in nature and was indexed to t-ZrO_2 and their planes are indicated in the insert of Fig. 8b.

4.7. *Phase stability analysis*

Fig. 9 revealed the XRD patterns of the annealed powders at 10 h, 50 h and 100 h, respectively. The low angle diffracted region (26°-36°) was usually made for the identification of m-phase and the use of high angle diffracted (400) region (71°-77°), can provide a distinction between tetragonal and cubic phase. It can be seen from Fig. 9a, that the powder particles exhibit excellent phase stability as the m-phase is absent even after heat treating for 100 h. In the (400) region, only tetragonal (004) and (400) peaks do exist and it does not contain any cubic phase. This conclusion is also supported by the deconvolution results, Fig. 10. It was reported that t phase along with c phase coexists after the thermal exposure [9,31–33]. Also, some other reports had shown the existence of multiple tetragonal phases along with or without cubic phase [8,34,35].

Hence, deconvolution (Lorentzian fit) of XRD patterns was carried out to identify the phases present after the heat treatment. Fig. 10 displays the deconvolution results, in 71°-77° region of powders annealed for 10 h (Fig. 10a) and 100 h (Fig. 10b) at 1573 K. It clearly shows that, there is no existence of c phase present along with the t phase, which demonstrates that the phase stability of t phase is better. The present result is in line with the report of Jones et al. [36]. When doping ZrO_2 with Gd^{3+} and Sm^{3+}, it produces substitutional defects and creates oxygen vacancies for charge compensation to maintain electroneutrality. Also, it may result in nanostructured defect clusters via stabilizer segregation [8,37], which reduces the concentration of single mobile defects [9]. At higher tem-

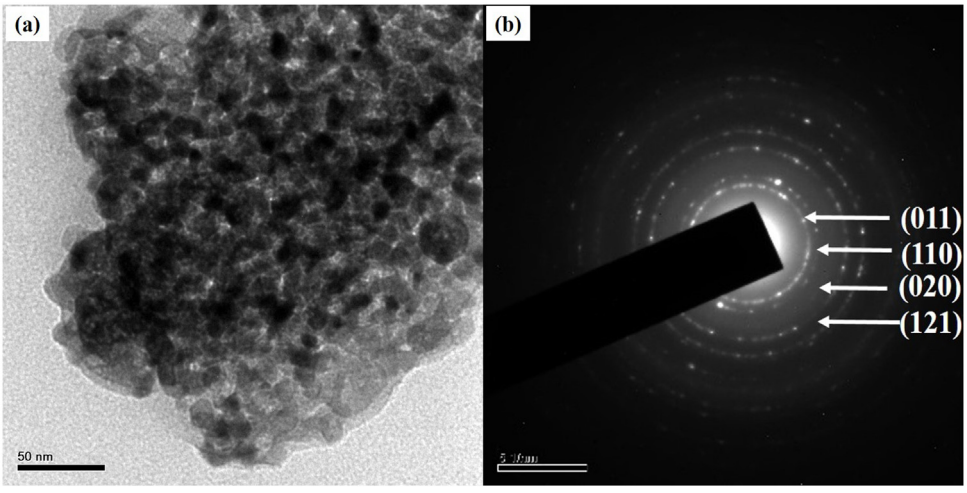

Fig. 8 – HR-TEM of 4Gd4SmSZ powders a) bright field image b) Selected Area Electron Diffraction pattern.

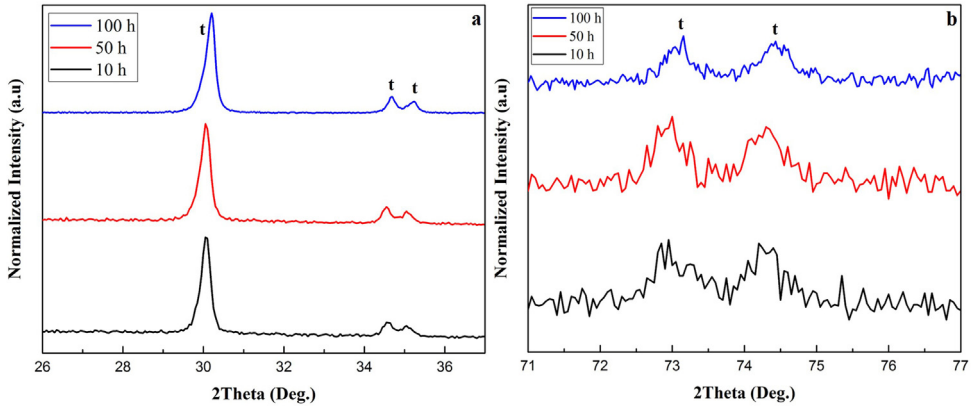

Fig. 9 – XRD pattern of 4Gd4SmSZ powders annealed at 1573 K a) low angle region b) high angle region.

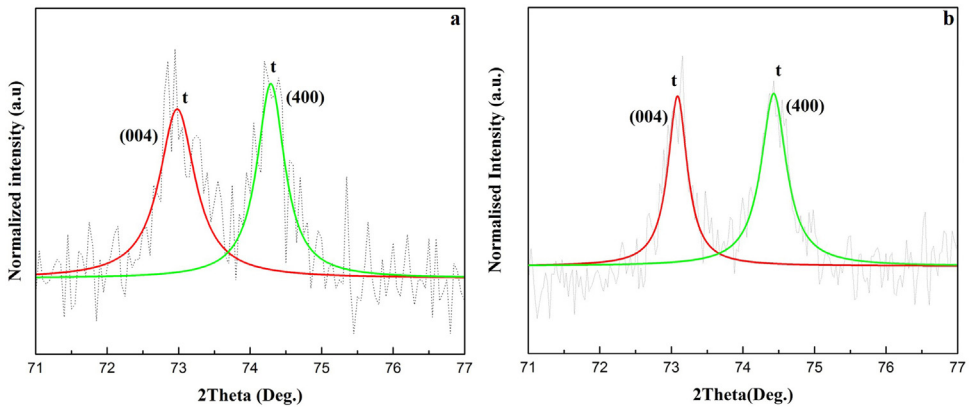

Fig. 10 – Deconvoluted (Lorentzian fit) XRD pattern of annealed 4Gd4SmSZ powders at 1573 K for 10 h b) 100 h showing tetragonal phase.

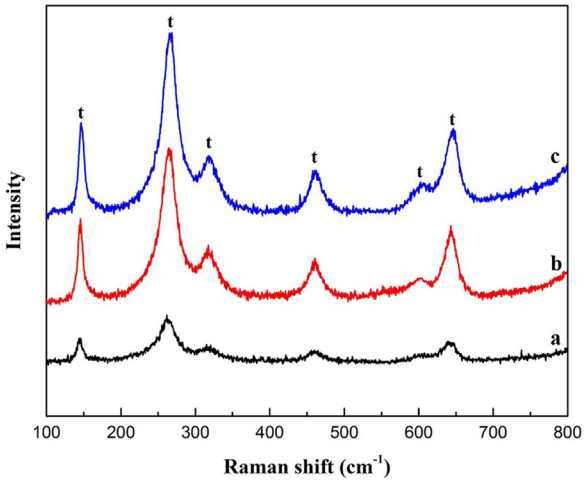

Fig. 11 – Raman spectra of annealed 4Gd4SmSZ powders at 1573 K for h b) 50 h and c) 100 h.

peratures, diffusion controlled process is responsible for the decomposition of t'phase to t and c phase and it requires long-range cation diffusion [8,32]. On cooling the stabilizer lean t phase transforms to m phase. However, the presence of defect clusters hinders the atomic mobility and mass transport at a higher temperature. As a result, it suppresses the diffusion of dopants into rich and lean regions, thus maintaining the t phase stability [32].

The obtained results of Raman spectra areshown in Fig. 11. Six distinct characteristic bands were observed at 145, 257, 365, 467, 608 and 642 cm^{-1} and they very well match with tetragonal polymorph. An increase in peak intensity with respect to annealing time was observed. As can be clearly seen, the most characteristic bands 178 and 189 cm^{-1} of monoclinic ZrO_2 were not present over the entire period of the experiment. The results of Raman spectroscopy are in good agreement with XRD result (Fig, 9a&b).

5. Conclusions

The ZrO_2-4 mol.% $GdO_{1.5}$-4 mol.% $SmO_{1.5}$ powders had retained tetragonal phase when calcined between 873 K to 1273 K for 2 h. The crystallite size increased from 11.97 nm to 13.28 nm at low temperature (873–1073 K) synthesis and from 13.28 nm to 18.90 nm(1073–1273 K) at higher temperature regime. The activation energy for the low temperature (873–1073 K) and high temperature (1073–1273 K) synthesis were found to be 4.04 kJ/mol. and20.04 kJ/mol. respectively. HR-TEM confirms the tetragonal nature. The 4Gd4SmSZ powders show better phase stability at 1573 K for 100 h.

REFERENCES

[1] Yu S, Wu Q, Azar MT, Liu CC. Sens Actuators B Chem 2002;85:212–8.
[2] Miura N, Jin H, Wama R, Nakakubo S, Elumalai P, Plashnitsa VV. Sens Actuators B Chem 2011;152:261–6.
[3] Kim HJ, Kim M, Neoh KC, Han GD, Bae K, Shin JM, et al. J.Pow. Sources 2016;327:401–7.
[4] Xu X, Xia C, Huang S, Peng D. Ceram Int 2005;31:1061–4.
[5] Liu H, Li S, Li Q, Li Y. Mater Des 2010;31:2972–7.
[6] Tsipas SA. J.Eur.Ceram. Soc 2010;30:61–72.
[7] Clarke DR. Surf Coat Technol 2003;163:67–74.
[8] Ponnuchamy MB, Gandhi AS. J Eur Ceram Soc 2015;35:1879–87.
[9] Sun L, Guo H, Peng H, Gong S, Xu H. Prog Nat Sci Mater Int 2013;23:440–5.
[10] Li QL, Cui XZ, Li SQ, Yang WH, Wang C, Cao Q. J Therm Spray Technol 2015;24:136–43.
[11] Loganathan A, Gandhi AS. Trans. IIM 2011;64:71–4.
[12] Hsu YW, Yang KH, Chang KM, Yeh SW, Wang MC. J Alloys Compd 2011;509:6864–70.
[13] Khollam YB, Deshpande AS, Patil AJ, Potdar HS, Deshpande SB, Date SK. Mater Chem Phys 2001;71:235–41.
[14] Juan IG, Ferrari B, Colomer MT. J Eur Ceram Soc 2009;29:3185–95.
[15] Huang W, Yang J, Meng X, Cheng Y, Wang C, Zou B, et al. Chem Eng J 2011;168:1360–8.
[16] Wang CL, Hwang WS, Chu HL, Yen FL, Hwang CY, His CS, et al. J Solgel Sci Technol 2014;70:428–40.

[17] Lopez T, Sanchez E, Bosch P, Meas Y, Gomez R. Mater Chem Phys 1992;32:141–52.
[18] Lee HE, Du JK, Sie YY, Wang CH, Wu JH, Wang CL, et al. J Non-Cryst Solids 2011;357:2103–8.
[19] Lee YH, Kuo CW, Hung IM, Fung KZ, Wang MC. J Non-Cryst. Solids 2005;351:3709–15.
[20] Sharma PK, Nass R, Schmidt H. Opt Mater (Amst) 1998;10:161–9.
[21] Richardson K, Akinc M. Ceram Int 1987;13:253–61.
[22] Kim DJ, Jung HJ, Yang IS. J Am Ceram Soc 1993;76:2106–8.
[23] Qu L, Choy KL. Ceram Int 2014;40:11593–9.
[24] Niu X, Xie M, Zhou F, Mu R, Song X, An S. J Mater Sci Technol 2014;30:381–6.
[25] Chraska T, King AH, Berndt CC. Mater Sci Eng A 2000;286:169–78.
[26] Hsu YW, Yang KH, Yeh SW, Wang MC. J Alloys Compd 2013;555:82–7.
[27] Chen SG, Yin YS, Wang DP, Li J. J Cryst Growth 2004;267:100–9.
[28] Wang CH, Wang MC, Du JK, Sie YY, Hsi CS, Lee HE. Ceram Int 2013;39:5165–74.
[29] Kuo CW, Lee KC, Yen FL, Shen YH, Lee HE, Wen SB, et al. J Alloys Compd 2014;592:288–95.
[30] Shukla S, Seal S, Vij R, Bandyopadhyay S. Nano Lett 2003;3:397–401.
[31] Zhao M, Ren X, Pan W. J Am Ceram Soc 2015;98:229–35.
[32] Liu H, Li S, Li Q, Li Y, Zhou W. Solid State Sci 2011;13:513–9.
[33] Sun L, Guo H, Peng H, Gong S, Xu H. Ceram Int 2013;39:3447–51.
[34] Jiang K, Liu S, Xi W. J Am Ceram Soc 2015;98:331–7.
[35] Lughi V, Clarke DR. Surf Coat Technol 2005;200:1287–91.
[36] Jones RL, Mess D. Surf Coat Technol 1996;86–87:94–101.
[37] Zhu DM, Chen YL, Miller RA. Ceram Eng Sci Proc 2003;24:525–34.